Available online at www.sciencedirect.com
SCIENCE DIRECT®
Journal of Computational Physics 192 (2003) 21–35
JOURNAL OF COMPUTATIONAL PHYSICS
www.elsevier.com/locate/jcp

Solving the two-body, bound-state Bethe–Salpeter equation ☆

G.B. Mainland

Department of Physics, The Ohio State University at Newark, Newark, OH 43055, USA

Received 22 August 2002; received in revised form 5 February 2003; accepted 2 July 2003

Abstract

By expanding the solution of the the two-body, bound-state Bethe–Salpeter equation in terms of basis functions that obey the boundary conditions, solutions can be obtained to some, if not many, equations that have heretofore proved intractable. The utility of choosing such basis functions is demonstrated by calculating the zero-energy, bound-state solutions of a spin-0 boson and a spin-1/2 fermion with unequal masses that interact via scalar electrodynamics and are described by the Bethe–Salpeter equation in the ladder approximation. The equation is solved by first making a Wick rotation and then projecting four-dimensional Euclidean space onto the surface of a unit, five-dimensional sphere. Solutions are expanded in terms of basis functions, each of which obeys the boundary conditions and can be expressed in terms of hyperspherical harmonics in five-dimensional space. The Bethe–Salpeter equation is discretized by requiring that the coefficient of each hyperspherical harmonic vanish. All integrations are performed analytically, yielding a generalized matrix eigenvalue equation that is solved numerically. Although the Bethe–Salpeter equation is separable in the zero-energy limit, the feature of Bethe–Salpeter equations that often prevents solutions from being obtained numerically is still present in the equation that is solved.

Keywords: Bethe–Salpeter equation; Bound-state equations

1. Introduction

There has been growing interest in solving relativistic, bound-state equations, both because important bound-state systems are relativistic and because the development of high-speed computers at least raises the possibility that such equations might be solved numerically. One physical problems that is of immediate interest is the constituent-quark models of mesons [1–4]. Properties of both light and heavy mesons have been calculated using equations that account for some relativistic effects.

While speculative, there is also interest in constituent models of leptons [5,6] and constituent models of quarks and leptons [7–11]. If the electron, muon, and tau are bound states of a single system, a severe constraint is imposed on the interaction and the structure of the composite system. The mass of the tau

☆ Supported by a grant from the Ohio Supercomputer Center.
E-mail address: mainland@mps.ohio-state.edu.

0021-9991/$ - see front matter
doi:10.1016/S0021-9991(03)00345-0

must, of course, be less than the sum of the masses of the bound, constituent particles. Since the ratio of the electron's mass to that of the tau's equals 1/3536, the mass of the electron must be less than 1/3536 of the sum of the constituent masses. Thus, the interaction must create a highly-relativistic, ultra-strongly bound state for which the binding energy is almost equal to the sum of the masses of the constituents. That is, the interaction must create a state that has almost zero energy. Similarly, if the positively- or negatively-charged quarks are bound states of a single system, the most tightly bound quark would necessarily almost be a zero-energy state.

A major reason that the Bethe–Salpeter equation [12] is not used more extensively is that, even numerically, the equation is extremely difficult to solve. To obtain numerical solutions, the equation is first discretized, and then the discretized equation, which is a generalized matrix eigenvalue equation, is solved numerically. Although the coupling constant is real in the Lagrangian, it is usually very difficult to discretize the Bethe–Salpeter equation in such a way that the calculated values of the coupling constant, which are eigenvalues of the generalized matrix eigenvalue equation, are both real and satisfy the Bethe–Salpeter equation. This problem can, at least sometimes if not often, be overcome by expanding the solution in terms of basis functions that obey the boundary conditions satisfied by the solution. The utility of choosing such basis functions is demonstrated by calculating the zero-energy, bound-state solutions of a spin-0 boson and a spin-1/2 fermion with unequal masses that interact via scalar electrodynamics and are described by the Bethe–Salpeter equation in the ladder approximation. To solve the equation, it is first Wick rotated [13] and then four-dimensional, Euclidean space is projected onto the surface of a unit, five-dimensional sphere. Solutions are expanded in terms of basis functions, each of which satisfies the boundary conditions and is expressed in terms of hyperspherical harmonics in five-dimensional space. The Bethe–Salpeter equation is discretized by requiring that the coefficient of each hyperspherical harmonic vanish. All integrations are performed analytically, yielding a generalized matrix eigenvalue equation that is solved numerically. Although the Bethe–Salpeter equation is separable in the zero-energy limit, the feature of the equation that usually prevents solutions from being obtained numerically is still present: It is not possible to construct a generalized matrix eigenvalue equation for which all eigenvalues are real. Nevertheless, the generalized matrix eigenvalue equation has some real eigenvalues, and these eigenvalues satisfy the Bethe–Salpeter equation.

Hyperspherical harmonics in (Euclidean) four-dimensional, space–time have previously been used to represent the angular dependence of solutions to the finite-energy, Bethe–Salpeter equation. As early as 1964, Schwartz [14] obtained bound-state solutions of two equal-mass scalars interacting through ϕ^3. More recently Setô and Fukui [15] obtained solutions for two unequal-mass scalars interacting through the exchange of a massive scalar, and Nieuwenhuis and Tijon [16] considered two equal-mass scalars interacting through the exchange of a massive scalar. In contrast, here solutions are expressed in terms of hyperspherical harmonics in five-dimensional space, so both the angular dependence and the momentum dependence of solutions are expressed in terms of hyperspherical harmonics.

The numerical method used here is an extension of an analytical method originally proposed by Sugano and Munakata [17] to obtain zero-energy, bound-state solutions of a spin-0 boson and a spin-1/2 fermion with equal masses that interact via scalar electrodynamics and are described by the Bethe–Salpeter equation in the ladder approximation. In that paper the solutions are expanded in terms of basis functions that can be expressed in terms of hyperspherical harmonics in five-dimensional space, but not all of the basis functions obey the boundary conditions. When their solutions are analyzed numerically by comparing the left- and right-hand sides of the equation at a set of widely separated momenta, the left- and right-hand sides of the equation are found to be unequal. Thus, the solutions are incorrect. Further analysis reveals that their proposed method for solving the equation fails because the series expansions for the solutions do not converge. The author made the same error when attempting to obtain zero-energy, bound-state solutions of a spin-0 boson and a spin-1/2 fermion with equal masses that interact via quantum electrodynamics [5]. In this paper it is demonstrated that when the expansions for solutions are written in terms of

basis functions that obey the boundary conditions, for the scalar electrodynamics model the expansions converge to solutions.

Numerical solutions to the bound-state, Bethe–Salpeter equation are typically obtained in three steps. (a) The singularity in the kernel is removed by a Wick rotation [13], which is accomplished by making the substitution $p_0 \to \mathrm{i}p_0$ and rotating the path of integration 90° counterclockwise in the complex p_0-plane. If the singularity is not removed, numerical solutions are exceedingly difficult to obtain [18]. (b) The Bethe–Salpeter equation is rotationally invariant in three-dimensional space if there are no external fields, so two angular variables can be separated. In the zero-energy limit the equation is rotationally invariant in four-dimensional space–time and can be completely separated. The resulting equation for the separated Bethe–Salpeter "wave function" $\Psi(|p|)$ is an equation in the variable $|p|$ where $|p| \equiv (p_0^2 + \mathbf{p}^2)^{1/2}$. In the ladder approximation a Wick-rotated, separated Bethe–Salpeter equation is of the form

$$K(|p|)\Psi(|p|) = \frac{g_1 g_2}{(2\pi)^4} \int_0^\infty \mathrm{d}|q| V(|p|,|q|)\Psi(|q|). \tag{1.1}$$

(c) Finally, the separated integral eigenvalue Eq. (1.1) for the coupling constant is discretized by converting it into a generalized matrix eigenvalue equation that is solved numerically. The discretization is typically achieved using one of the following two methods:

To implement the Rayleigh–Ritz–Galerkin method (see, for example, [19,20]), the Bethe–Salpeter "wave function" $\Psi(|p|)$ is expressed in terms of a set of basis functions $\{B_j(|p|)\}$,

$$\Psi(|p|) = \sum_{j=1}^{N} c_j B_j(|p|). \tag{1.2}$$

After multiplying (1.1) by $B_i(|p|)^\dagger$ and integrating over the variable $|p|$, the integral equation is converted into a generalized matrix eigenvalue equation,

$$Kc = \frac{g_1 g_2}{(2\pi)^4}(V_{\mathrm{H}} + V_{\mathrm{AH}})c. \tag{1.3}$$

In the above equation, c is a column vector with the elements c_j that are the expansion coefficients for the wave function $\Psi(|p|)$ in (1.2), and the matrices V_{H} and V_{AH} are Hermitian and anti-Hermitian, respectively.

To implement the collocation method [19,20], the solution $\Psi(|p|)$ is also expanded in terms of basis functions as given in (1.2). The Bethe–Salpeter equation is then converted into a generalized matrix eigenvalue equation of the form (1.3) by requiring that the left- and right-hand sides of the equation agree at N widely-distributed values of momentum $|p|$.

In general it is extremely difficult to formulate (1.3) in such a way that the coupling constant $g_1 g_2/(2\pi)^4$, which is calculated as an eigenvalue, is forced to be real. A sufficient condition for obtaining real eigenvalues of a generalized matrix eigenvalue Eq. (1.3) is that $V_{\mathrm{AH}} = 0$, K be Hermitian and either K or V_{H} be positive definite [21]. Somewhat different matrix Eq. (1.3) can be constructed from a Bethe–Salpeter Eq. (1.1), and this freedom can sometimes be used to convert the Bethe–Salpeter eigenvalue equation into a generalized matrix eigenvalue equation that yields real eigenvalues.

In this paper a third method, the method of orthogonal functions, is used to discretize and solve the separated Bethe–Salpeter equation. The solution is expanded in terms of a complete set of basis functions $\{B_j(|p|)\}$ where each basis function satisfies the boundary conditions and is a linear combination of orthogonal functions $\{P_j(|p|)\}$. Thus,

$$B_j(|p|) = \sum_{k=1}^{N_j} b_{j,k} P_k(|p|), \tag{1.4}$$

where the $b_{j,k}$ are chosen so that $B_j(|p|)$ satisfies the boundary conditions. Expressing the solution $\Psi(|p|)$ in terms of the $B_j(|p|)$ as given in (1.4), (1.1) becomes

$$K(|p|)\sum_{j=1}^{N}\sum_{k=1}^{N_j} c_j b_{j,k} P_k(|p|) = \frac{g_1 g_2}{(2\pi)^4}\sum_{j=1}^{N}\sum_{k=1}^{N_j}\int_0^\infty \mathrm{d}|q| V(|p|,|q|) c_j b_{j,k} P_k(|q|). \tag{1.5}$$

When the orthogonal functions $P_j(|p|)$ are chosen to be spherical functions (hyperspherical harmonics with the four-dimensional angular dependence separated), the integral on the right-hand side of (1.5) can be evaluated analytically and expressed as a sum of spherical functions. Eq. (1.5) is then solved by requiring the equality of the coefficient of each spherical function on the left- and right-hand sides. The striking feature of this method, when it is used to solve the Bethe–Salpeter equation describing a bound state of a spin-0 boson and a spin-1/2 fermion interacting via scalar electrodynamics, is as follows: Although the resulting generalized matrix equation is of the form (1.3) and all of the eigenvalues are not forced to be real, real eigenvalues are obtained. Furthermore, when a sufficiently large number of basis functions are used, for each real eigenvalue the corresponding series (1.2) converges to a solution of the Bethe–Salpeter equation.

2. The Bethe–Salpeter equation: separation and boundary conditions

When a spin-0 field $\phi(x)$, which represents a scalar with mass m_s, and a spin-1/2 field $\Psi(x)$, which represents a fermion with mass m_f, interact via scalar electrodynamics, represented by the massless, scalar field A, the renormalizable interaction Lagrangian is

$$L_\mathrm{int} =: g_1 \bar{\Psi} A \Psi + g_2 \phi^\dagger A \phi : . \tag{2.1}$$

(The notation is that of [22]. The constants $\hbar$ and c are set to unity. Repeated Greek indices are summed from 0–3 and repeated Roman indices are summed from 1–3. Bold variables represent vectors in three-dimensional space.) Following standard procedures [12], in the ladder approximation and in the zero-energy limit, the Bethe–Salpeter equation describing a bound state of a spin-0 boson and a spin-1/2 fermion is

$$(p^\mu \gamma_\mu - m_\mathrm{f})(p^\mu p_\mu - m_\mathrm{s}^2)\chi(p) = \frac{\mathrm{i}g_1 g_2}{(2\pi)^4}\int_{-\infty}^{\infty}\frac{\mathrm{d}^4 q}{(p-q)^2 + \mathrm{i}\epsilon}\chi(q). \tag{2.2}$$

Performing a Wick rotation [13], (2.2) becomes

$$(\tilde{\gamma}\cdot p + m_\mathrm{f})(p\cdot p + m_\mathrm{s}^2)\Psi(p) = \frac{g_1 g_2}{(2\pi)^4}\int_{-\infty}^{\infty}\frac{\mathrm{d}^4 q}{(p-q)\cdot(p-q)}\Psi(q). \tag{2.3}$$

In the above equation $\Psi(p) \equiv \chi(\mathrm{i}p^0, \mathbf{p})$, the Euclidean scalar product $p\cdot p \equiv p^0 p^0 + \mathbf{p}\cdot\mathbf{p}$ and $\tilde{\gamma}\cdot p \equiv \tilde{\gamma}^0 p^0 + \tilde{\gamma}^\mathrm{i} p^\mathrm{i}$. The matrices $\tilde{\gamma}^\mu$ are given by $\tilde{\gamma}^0 \equiv -\mathrm{i}\gamma^0$, $\tilde{\gamma}^\mathrm{i} \equiv \gamma^\mathrm{i}$.

Dimensionless variables are introduced by defining $m_\mathrm{f} \equiv m(1-\Delta)$, $m_\mathrm{s} \equiv m(1+\Delta)$, $p' \equiv p/m$ and $q' \equiv q/m$. Writing (2.3) in terms of dimensionless variables and omitting primes since all momenta are now dimensionless,

$$[\tilde{\gamma}\cdot p + (1-\Delta)][p\cdot p + (1+\Delta)^2]\Psi(p) = \frac{g_1 g_2}{(2\pi)^4 m}\int_{-\infty}^{\infty}\frac{\mathrm{d}^4 q}{(p-q)\cdot(p-q)}\Psi(q). \tag{2.4}$$

Spherical coordinates are introduced as follows:

$$\begin{aligned} p^0 &= |p|\cos\theta_2, \\ p_z &= |p|\sin\theta_2\cos\theta_3, \\ p_x &= |p|\sin\theta_2\sin\theta_3\sin\phi, \\ p_y &= |p|\sin\theta_2\sin\theta_3\cos\phi. \end{aligned} \tag{2.5}$$

The four-vector q is written similarly in terms of primed angles. Then

$$\mathrm{d}^4q = |q|^3\sin^2\theta_2'\sin\theta_3'\,\mathrm{d}\theta_2'\,\mathrm{d}\theta_3'\,\mathrm{d}\phi'\,\mathrm{d}|q| \equiv |q|^3\,\mathrm{d}|q|\,\mathrm{d}\Omega_{(3)}' \tag{2.6}$$

and

$$(p-q)\cdot(p-q) = |p|^2 + |q|^2 - 2|p||q|\cos\Theta, \tag{2.7}$$

where Θ is the angle between the vectors p and q.

The Bethe–Salpeter equation separates into two coupled equations in the variable $|p|$ when the solution is written in the form

$$\Psi^{(\pm)}(p) = \mathscr{F}^{(\pm)}(|p|)\Psi_1^{(\pm)}(\theta_2,\theta_3,\phi) + \mathscr{G}^{(\pm)}(|p|)\Psi_2^{(\pm)}(\theta_2,\theta_3,\phi). \tag{2.8}$$

The four-component column vectors $\Psi_1^{(\pm)}$ and $\Psi_2^{(\pm)}$, which are defined in [5], have components that are hyperspherical harmonics in four-dimensional space and are related as follows:

$$\Psi_1^{(-)} = \gamma_5\Psi_1^{(+)} \quad \text{and} \quad \Psi_2^{(-)} = \gamma_5\Psi_2^{(+)}. \tag{2.9}$$

The functions $\Psi_1^{(\pm)}$ and $\Psi_2^{(\pm)}$satisfy the relationships

$$\tilde{\gamma}\cdot p\Psi_1^{(\pm)} = \mp|p|\Psi_2^{(\pm)} \quad \text{and} \quad \tilde{\gamma}\cdot p\Psi_2^{(\pm)} = \pm|p|\Psi_1^{(\pm)}. \tag{2.10}$$

After substituting $\Psi^{(+)}(p)$ as given in (2.8) into the Bethe–Salpeter Eq. (2.4), the left-hand side can be simplified using (2.10), and the angular integration on the right-hand side can be performed using Hecke's theorem [23]. (All formulas necessary for carrying out the angular integration are given in the appendix of [5].) The coefficients of $\Psi_1^{(+)}(\theta_2,\theta_3,\phi)$ and $\Psi_2^{(+)}(\theta_2,\theta_3,\phi)$ must vanish independently, yielding the following two separated, coupled equations:

$$\begin{aligned} &\left[|p|^2 + (1+\Delta)\right]^2\left[(1-\Delta)F^{(+)}(|p|) + |p|G^{(+)}(|p|)\right] \\ &\quad = \frac{g_1g_2}{(2\pi)^4 m}\int_0^\infty |q|^3\Delta^{(2)}_{k_1-\frac{1}{2}}(|p|,|q|)F^{(+)}(|q|)\mathrm{d}|q|, \end{aligned} \tag{2.11a}$$

$$\begin{aligned} &\left[|p|^2 + (1+\Delta)\right]^2\left[-|p|F^{(+)}(|p|) + (1-\Delta)G^{(+)}(|p|)\right] \\ &\quad = \frac{g_1g_2}{(2\pi)^4 m}\int_0^\infty |q|^3\Delta^{(2)}_{k_1+1/2}(|p|,|q|)G^{(+)}(|q|)\mathrm{d}|q|. \end{aligned} \tag{2.11b}$$

In the above equation the index $k_1 = 1/2, 3/2, \ldots$ and

$$\Delta_n^{(2)}(|p|,|q|) = \frac{2\pi^2}{|p||q|}\,\frac{R(|p|,|q|)^{n+1}}{n+1}, \tag{2.12a}$$

where

$$R(|p|,|q|) = \begin{cases} \frac{|q|}{|p|} & \text{if } |q| \leqslant |p|, \\ \frac{|p|}{|q|} & \text{if } |q| \geqslant |p|. \end{cases} \tag{2.12b}$$

When $\Psi^{(-)}(p)$ as given in (2.8) is substituted into the Bethe–Salpeter Eq. (2.4), the two equations that are obtained are identical to (2.11) after making the substitutions $F^{(+)}(|p|) \to F^{(-)}(|p|)$ and $G^{(+)}(|p|) \to -G^{(-)}(|p|)$. Since no additional eigenvalues are obtained by considering this second set of equations, attention is restricted to (2.11), and the superscripts (+) are dropped for $F^{(+)}(|p|)$ and $G^{(+)}(|p|)$.

The boundary conditions as $|p|$ approaches zero and infinity are readily obtained from the separated (2.11) and the asymptotic properties of $\Lambda_n^{(2)}(|p|,|q|)$ that immediately follow from (2.12):

$$\Lambda_n^{(2)}(|p|,|q|) \underset{|p|\to 0}{\to} |p|^n, \tag{2.13a}$$

$$\Lambda_n^{(2)}(|p|,|q|) \underset{|p|\to \infty}{\to} \frac{1}{|p|^{n+2}}. \tag{2.13b}$$

As $|p|$ approaches zero, the functions $F(|p|)$ and $G(|p|)$ have the asymptotic properties

$$F(|p|) \underset{|p|\to 0}{\to} |p|^f \quad \text{and} \quad G(|p|) \underset{|p|\to 0}{\to} |p|^g, \tag{2.14}$$

where the constants f and g must be determined. Using (2.13a) and (2.14), at small $|p|$ (2.11) becomes

$$(1+\Delta)^2 \begin{bmatrix} (1-\Delta)|p|^f + |p|^{g+1} \\ -|p|^{f+1} + (1-\Delta)|p|^g \end{bmatrix} \sim \frac{g_1 g_2}{m} \begin{bmatrix} |p|^{k_1-1/2} \\ |p|^{k_1+1/2} \end{bmatrix}. \tag{2.15}$$

Eq. (2.15) is satisfied at small $|p|$ provided

$$f = k_1 - \frac{1}{2} \quad \text{and} \quad g \geqslant k_1 + \frac{1}{2}. \tag{2.16}$$

As $|p|$ approaches infinity, the functions $F(|p|)$ and $G(|p|)$ have the asymptotic properties

$$F(|p|) \underset{|p|\to \infty}{\to} \frac{1}{|p|^{f'}} \quad \text{and} \quad G(|p|) \underset{|p|\to \infty}{\to} \frac{1}{|p|^{g'}}. \tag{2.17}$$

Substituting (2.17) into (2.11) and solving the equation in the limit of large $|p|$ yields

$$f' \geqslant k_1 + \frac{11}{2} \quad \text{and} \quad g' = k_1 + \frac{9}{2}. \tag{2.18}$$

3. Numerical solution of the Bethe–Salpeter equation

The separated Bethe–Salpeter (2.11) is solved numerically using a method that is a generalization of the unsuccessful analytical procedure originally proposed by Sugano and Munakata [17]. The method used here is similar to that proposed in [17] in that solutions are expressed as sums of hyperspherical harmonics in five-dimensional Euclidean space and that all integrations are performed analytically using Hecke's theorem [23]. The major differences are as follows: (1) Solutions are expanded in terms of basis functions, each of which satisfies the boundary conditions. (2) To analytically integrate the terms in the expansion for $G(|p|)$, $G(|p|)$ must be reexpressed in terms of a series with two indices that independently range to infinity. (3) The resulting matrix equation yields solutions both when the constituent masses are

equal and unequal. (4) The equation is solved numerically and does not appear to be readily solvable analytically.

To solve the equation, four-dimensional momentum space is projected onto the surface of a unit, five-dimensional sphere,

$$|p| = \tan(\theta_1/2) = \sqrt{\frac{1-z}{1+z}}, \quad z \equiv \cos\ \theta_1, \tag{3.1}$$

a procedure originally proposed by Fock [24] and elaborated on by Lévy [25]. In this five-dimensional space, hyperspherical harmonics Y_μ are of the form

$$Y_\mu = P^{(3)}_{\mu,p_1}(\cos\theta_1) P^{(2)}_{p_1,p_2}(\cos\theta_2) P^{(1)}_{p_2,p_3}(\cos\theta_3) \mathrm{e}^{\pm \mathrm{i} p_3 \phi}, \tag{3.2}$$

where the integers μ, p_1, p_2, and p_3 satisfy the conditions $\mu \geqslant p_1 \geqslant p_2 \geqslant p_3 \geqslant 0$. In (3.2) the spherical functions $P^{(s)}_{i,j}(z)$ are given by [5]

$$P^{(s)}_{i,j}(z) = (1-z^2)^{j/2} \frac{\mathrm{d}^j}{\mathrm{d}z^j} C_i^{s/2}(z). \tag{3.3}$$

The $C_i^{s/2}(z)$ in (3.3) are Gegenbauer polynomials.

Solutions are sought that are of the form

$$F(|p|) \sim \sum_{n=0}^{N} f_n (1-z)^{n_f} (1+z)^{n'_f} P^{(3)}_{n+k_1-\frac{1}{2},k_1-\frac{1}{2}}(z) \tag{3.4a}$$

and

$$G(|p|) \sim \sum_{n=0}^{N} g_n (1-z)^{n_g} (1+z)^{n'_g} P^{(3)}_{n+k_1+\frac{1}{2},k_1+\frac{1}{2}}(z). \tag{3.4b}$$

The final indices $k_1 \pm 1/2$ in $P^{(3)}_{i,k_1\pm1/2}(z)$ in (3.4a) and (3.4b) are chosen, respectively, so that each term in the expansion of the solution is a hyperspherical harmonic. Since from (3.3), $P^{(3)}_{i,j}(z) = 0$ for $i < j$, the sums over n in (3.4) have been restricted to include only non-zero terms. The constants n_f, n_g, $n_{f'}$, and $n_{g'}$ are now chosen so that each of the basis functions in (3.4) obeys the boundary conditions. Since no additional solutions were found when the parameter g in (2.16) was greater than $k_1 + 1/2$ or when f' in (2.18) was greater than $k_1 + 11/2$, those cases will not be considered here.

From definition (3.3) of $P^{(3)}_{i,j}(z)$, for z near ± 1,

$$P^{(3)}_{i,j}(z) \sim (1-z^2)^{j/2}. \tag{3.5}$$

From (2.14) and (2.16), for small momenta $|p|$, $F(|p|) \sim |p|^{k_1-1/2}$. Requiring that the basis functions in (3.4a) have this same behavior at small $|p|$ yields the equation

$$F(|p|) \sim |p|^{k_1-1/2} \sim (1-z)^{(k_1-1/2)/2} \sim (1-z)^{n_f}(1-z)^{(k_1-1/2)/2}, \tag{3.6}$$

which has the solution $n_f = 0$. The remaining three constants are determined in a similar fashion with the result

$$n_f = 0, \quad n_g = 0, \quad n_{f'} = 3, \quad n_{g'} = 2. \tag{3.7}$$

As a consequence of (3.7), solutions are sought that are of the form

$$F(|p|) = \sum_{n=0}^{N} f_n (2n + 2k_1 + 2) \cos^6(\theta_1/2) P^{(3)}_{n+k_1-\frac{1}{2},k_1-\frac{1}{2}}(z), \tag{3.8a}$$

$$G(|p|) = \sum_{n=0}^{N} g_n (2n + 2k_1 + 4) \cos^4(\theta_1/2) P^{(3)}_{n+k_1+\frac{1}{2},k_1+\frac{1}{2}}(z). \tag{3.8b}$$

Eqs. (3.8) differ from (3.4) by constants that have been included for calculational convenience. With the aid of an identity in the appendix of [5], each basis function can be rewritten as a sum of spherical functions, so the basis functions in 3.8 are of the form (1.4). Sugano and Munakata [17] essentially used the expansions (3.8) except that in (3.8b), $\cos^4(\theta_1/2)$ is replaced by $\cos^6(\theta_1/2)$ so that the basis functions in (3.8b) do not satisfy the boundary conditions satisfied by $G(|p|)$.

The unit vector $\hat{u}$ in five-dimensional space is defined by

$$\hat{u} \equiv (\cos\theta_1, \sin\theta_1 \cos\theta_2, \sin\theta_1 \sin\theta_2 \cos\theta_3, \sin\theta_1 \sin\theta_2 \sin\theta_3 \cos\phi, \sin\theta_1 \sin\theta_2 \sin\theta_3 \sin\phi). \tag{3.9}$$

Defining the momentum $|q|$ and the unit vector $\hat{v}$ as in (3.1) and (3.9), respectively, except in terms of primed angles,

$$\frac{1}{(p-q)^2} = \frac{\cos^2\frac{\theta_1}{2} \cos^2\frac{\theta_1'}{2}}{\frac{1}{2}(1 - \cos\Theta)}, \tag{3.10}$$

where Θ is the angle between the unit vectors $\hat{u}$ and $\hat{v}$, and

$$\mathrm{d}^4 q = \frac{\sin^3\theta_1' \sin^2\theta_2' \sin\theta_3' \mathrm{d}\theta_1' \mathrm{d}\theta_2' \mathrm{d}\theta_3' \mathrm{d}\phi'}{16\cos^8(\theta_1'/2)} \equiv \frac{\mathrm{d}\Omega'_{(4)}}{16\cos^8(\theta_1'/2)}. \tag{3.11}$$

Using the above results to write the Bethe–Salpeter Eq. (2.4) in terms of angular variables,

$$\begin{aligned}
&\frac{1}{2}\left[\Delta^2 + 2\Delta + 2 + \Delta(\Delta+2)z\right]\Bigg\{\left[\frac{1}{2}(1+z)\right]^2 (1-\Delta) \sum_{n=0}^{N} f_n (2n + 2k_1 + 2) P^{(3)}_{n+k_1-\frac{1}{2},k_1-\frac{1}{2}}(z) \Psi_1^{(+)}(\theta_2, \theta_3, \phi) \\
&\quad + \frac{1}{2}\sqrt{1-z^2} \sum_{n=0}^{N} g_n (2n + 2k_1 + 4) P^{(3)}_{n+k_1+\frac{1}{2},k_1+\frac{1}{2}}(z) \Psi_1^{(+)}(\theta_2, \theta_3, \phi) - \frac{1}{2}\cos^2(\theta_1/2)\sqrt{1-z^2} \\
&\quad \times \sum_{n=0}^{N} f_n (2n + 2k_1 + 2) P^{(3)}_{n+k_1-\frac{1}{2},k_1-\frac{1}{2}}(z) \Psi_2^{(+)}(\theta_2, \theta_3, \phi) + \cos^2(\theta_1/2)(1-\Delta) \\
&\quad \times \sum_{n=0}^{N} g_n (2n + 2k_1 + 4) P^{(3)}_{n+k_1+\frac{1}{2},k_1+\frac{1}{2}}(z) \Psi_2^{(+)}(\theta_2, \theta_3, \phi)\Bigg\} \\
&\qquad = \cos^2(\theta_1/2) \frac{g_1 g_2}{(4\pi)^4 m} \int \frac{\mathrm{d}\Omega'_{(4)}}{\frac{1}{2}(1 - \cos\Theta)} \Bigg\{ \sum_{n=0}^{N} f_n (2n + 2k_1 + 2) P^{(3)}_{n+k_1-\frac{1}{2},k_1-\frac{1}{2}}(z') \Psi_1^{(+)}(\theta_2', \theta_3', \phi') \\
&\qquad\quad + \frac{1}{\cos^2(\theta_1'/2)} \sum_{n=0}^{N} g_n (2n + 2k_1 + 4) P^{(3)}_{n+k_1+\frac{1}{2},k_1+\frac{1}{2}}(z') \Psi_2^{(+)}(\theta_2', \theta_3', \phi') \Bigg\}.
\end{aligned} \tag{3.12}$$

Each term in the first sum on the right-hand side of (3.12) is a hyperspherical harmonic so the integral over each term can immediately be evaluated using Hecke's theorem [25]. (All necessary formulas are in the appendix of [5].) Because the factor $1/\cos^2(\theta_1'/2)$ multiplies the second sum on the right-hand side of (3.12),

each term is not a hyperspherical harmonic. However, it is possible to rewrite the second sum in terms of hyperspherical harmonics using the expansion

$$\frac{1}{\cos^2(\theta_1/2)}P^{(3)}_{i,r}(z) = \sum_{k=1}^{\infty} a^{(3)}_{i,r,k} P^{(3)}_{k-1+r,r}(z). \tag{3.13}$$

In Appendix A the expansion parameter $a^{(3)}_{i,r,1}$ is calculated explicitly and a recursion relation is derived that allows the calculation of all remaining expansion parameters $a^{(3)}_{i,r,k}$, $k \geqslant 2$. Using (3.13) the second term on the right-hand side of (3.12) can now be integrated using Hecke's theorem. The coefficients of $\Psi^{(+)}_1$ and $\Psi^{(+)}_2$ must vanish independently, yielding two coupled, algebraic equations. Multiplying both equations by four and cancelling the common factor of $\cos^2(\theta_1/2)$ in the second equation,

$$\begin{aligned}
&\left[\Delta^2 + 2\Delta + 2 + \Delta(\Delta+2)z\right]\left\{\frac{1}{2}(1+z)^2(1-\Delta)\sum_{n=0}^{N} f_n(2n+2k_1+2)P^{(3)}_{n+k_1-\frac{1}{2},k_1-\frac{1}{2}}(z)\right.\\
&\quad\left. + \sqrt{1-z^2}\sum_{n=0}^{N} g_n(2n+2k_1+4)P^{(3)}_{n+k_1+\frac{1}{2},k_1+\frac{1}{2}}(z)\right\}\\
&\qquad = \frac{g_1 g_2}{128\pi^4 m}(1+z)\sum_{n=0}^{N} f_n(2n+2k_1+2)\Delta^{(3)}_{n+k_1-\frac{1}{2}} P^{(3)}_{n+k_1-\frac{1}{2},k_1-\frac{1}{2}}(z),
\end{aligned} \tag{3.14a}$$

$$\begin{aligned}
&\left[\Delta^2 + 2\Delta + 2 + \Delta(\Delta+2)z\right]\left\{-\sqrt{1-z^2}\sum_{n=0}^{N} f_n(2n+2k_1+2)P^{(3)}_{n+k_1-\frac{1}{2},k_1-\frac{1}{2}}(z)\right.\\
&\quad\left. + 2(1-\Delta)\sum_{n=0}^{N} g_n(2n+2k_1+4)P^{(3)}_{n+k_1+\frac{1}{2},k_1+\frac{1}{2}}(z)\right\}\\
&\qquad = \frac{g_1 g_2}{64\pi^4 m}\sum_{n=0}^{N}\sum_{k=1}^{\infty} g_n(2n+2k_1+4)\times a^{(3)}_{n+k_1+\frac{1}{2},k_1+\frac{1}{2},k}\Delta^{(3)}_{k+k_1-\frac{1}{2}} P^{(3)}_{k+k_1-\frac{1}{2},k_1+\frac{1}{2}}(z).
\end{aligned} \tag{3.14b}$$

In the above equations, the factor $\Delta^{(3)}_n = 16\pi^2/(n+1)(n+2)$ (see [5]) occurs when the integration is performed using Hecke's theorem.

Using identities in [5], the factors of z and $\sqrt{1-z^2}$ in (3.14) can be eliminated with the result that the only functions that occur in (3.14a) and (3.14b) are of the form $P^{(3)}_{i,k_1-1/2}(z)$ and $P^{(3)}_{i,k_1+1/2}(z)$, respectively. Eq. (3.14) is discretized by truncating the expansion (3.13) and requiring that the coefficient of each spherical function $P^{(3)}_{i,k_1\pm1/2}(z)$ vanish. The resulting generalized matrix eigenvalue equation is of the form (1.3), but the matrix K is not Hermitian, V_{AH} is not zero and neither K nor $V_{\mathrm{H}} + V_{\mathrm{AH}}$ is positive definite. All of the eigenvalues are not forced to be real and, in fact, all are not. Nevertheless, solutions are obtained with real eigenvalues.

When z or $\sqrt{1-z^2}$ multiplies a spherical function $P^{(3)}_{i,j}(z)$, one spherical function that results has an index $i \to i+1$. Therefore, when a finite number of basis functions are used, there are more different spherical functions in the equations than there are expansion parameters. Thus, a solution is not obtained unless the expansion parameters f_n and g_n go to zero sufficiently fast that the expansions converge. When a sufficient number of basis functions are used, for each real eigenvalue, the expansions for the corresponding solution converge so that the solution does in fact satisfy the Bethe–Salpeter equation.

As the value of the mass-ratio parameter Δ decreases to -1.0, larger numbers of basis functions are required to calculate accurate eigenvalues $g_1 g_2/(8\pi^2 m)$: When $k_1 = 1/2$ and solutions are expanded in terms of 25 basis functions, eigenvalues are stable to four or five significant figures in the region $-0.72 \leqslant \Delta$. To

obtain comparable accuracy when $\Delta = -0.98$, 150 basis functions are required, and when $\Delta < -0.995$, some eigenvalues are accurate only to one or two significant figures when solutions are expanded in terms of 450 basis functions. In Figs. 1 and 2, values of $g_1 g_2/(8\pi^2 m)$ graphed with dashed lines indicate that (eigen)values may not be accurate to three significant figures. In addition to the three graphed solutions, other solutions apparently exist in the region $-1 \leqslant \Delta \leqslant -0.995$, but the series expansions do not converge sufficiently well in the region to determine accurate eigenvalues.

As a consequence of the rotational symmetry in four-dimensional space–time, solutions with the same value of k_1 but different values of angular momentum j are degenerate. From (3.2), $k_1 \geqslant j$, so the solutions in Fig. 1 have angular momentum $j = 1/2$. Similarly, there are degenerate $j = 1/2$ and $j = 3/2$ solutions with $k_1 = 3/2$ as shown in Fig. 2.

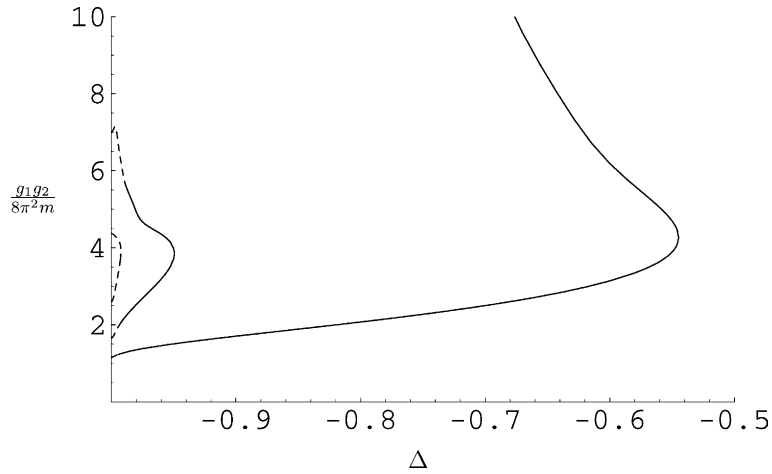

Fig. 1. The coupling constant $g_1 g_2/(8\pi^2 m)$ as a function of the mass-ratio parameter Δ when $k_1 = 1/2$.

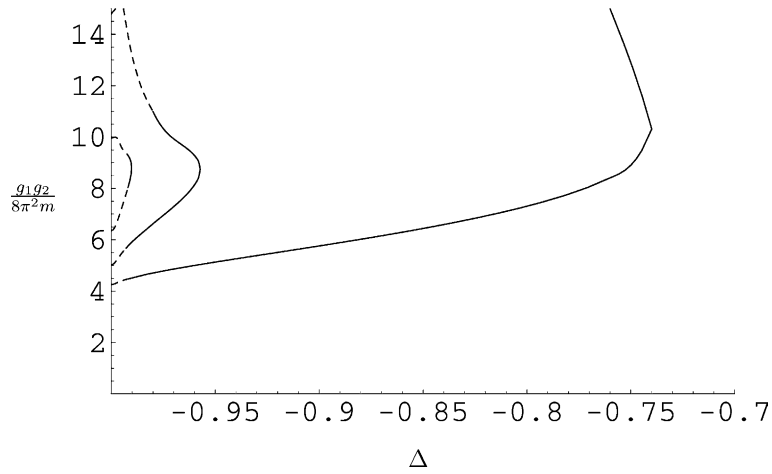

Fig. 2. The coupling constant $g_1 g_2/(8\pi^2 m)$ as a function of the mass-ratio parameter Δ when $k_1 = 3/2$.

A typical solution for $F(|p|)$ and $G(|p|)$, with a corresponding eigenvalue $g_1g_2/(8\pi^2m) = 2.4986$, is graphed in Fig. 3. The normalization of $F(|p|)$ and $G(|p|)$ is arbitrary, but the same. Note that the vertical scales are different for the two graphs, and that the maximum value of $F(|p|)$ is much larger than that of $G(|p|)$. From Fig. 3 it is immediately obvious that $F(|p|)$ and $G(|p|)$ satisfy the boundary conditions (2.16) as $|p| \to 0$: $F(|p|)$ is constant at small $|p|$ and $G(|p|)$ grows linearly. The behavior of the solutions as $|p| \to \infty$ is that expected from (2.18): Although too small to be seen in Fig. 3, $F(|p|)$ becomes negative near $|p| \simeq 4$ and then approaches zero from below as $1/|p|^6$. At large $|p|$ the solution $G(|p|)$ approaches zero as $1/|p|^5$. If such a solution were intended to describe an actual physical state, the large value of $g_1g_2/(8\pi^2m)$ implies that higher-order diagrams are important and, perhaps, even suggests that the perturbative approach is inappropriate.

To check for errors in the matrix eigenvalue equation, each matrix element was calculated using two rather different methods. First they were calculated directly from (3.14). Then using the orthogonality relation

$$\int_{-1}^{1} \mathrm{d}z(1-z^2)^{(s-1)/2} P_{i,j}^{(s)}(z) P_{i',j}^{(s)}(z) = \frac{\pi\Gamma(i+j+s)}{2^{s-2}(2i+s)\Gamma(i-j+1)\Gamma^2(s/2)}\delta_{i,i'} \equiv \frac{1}{\tilde{N}_{i,j}^{(s)}}\delta_{i,i'}, \tag{3.15}$$

the matrix elements were calculated from (2.11). Specifically, to calculate the coefficient of $P^{(3)}_{KF_{\min}-1+i,k_1-1/2}(z)$, (2.11a) is multiplied by $\tilde{N}^{(3)}_{KF_{\min}-1+i,k_1-1/2}(1-z^2)P^{(3)}_{KF_{\min}-1+i,k_1-1/2}(z)$ and then integrated over the variable z. The parameter $KF_{\min}$ is the minimum value of the index j in $P^{(3)}_{j,k_1-1/2}(z)$ that appears in (2.11a), and $i = 1, 2, \ldots, N$. $KF_{\min}$ is calculated analytically by determining how many times the functions in the equation lower the first index of the spherical functions that are in the expansions for solutions and recalling that $P^{(s)}_{i,j}(z) = 0$ if $i < j$. The coefficients of $P^{(3)}_{KG_{\min}-1+i,k_1+1/2}(z)$ are similarly calculated from (2.11b). The single integration on the left-hand side of the equations and the double integration on the right-hand sides are performed numerically using Gaussian quadrature with a seven point option between each knot.

Even though the solutions are calculated from (3.14), they are checked using (2.11), thereby providing a check of both the steps leading from (2.11) to (3.14) as well as a check of the solutions. For each solution the left- and right-hand sides of the equations are calculated and compared at momenta $|p|$ corresponding to $\mathcal{N} = 20$ Chebychev points z. A reliability coefficient $r_{\text{lhs–rhs}}$, which is a statistical measure of how well the left- and right-hand sides of the equations agree at $\mathcal{N}$ widely-distributed values of momenta $p_1, \ldots, p_{\mathcal{N}}$, is then calculated. Letting LHS_i^a and RHS_i^a be, respectively, the values of the left- and right-hand sides of (2.11a) at the value of momentum p_i, with corresponding expressions for the left- and right-hand sides of (2.11b), the reliability coefficient is [26]

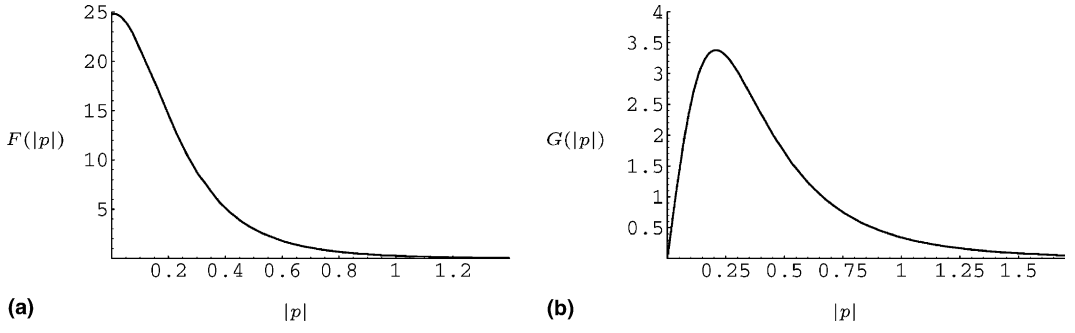

Fig. 3. The solutions (a) $F(|p|)$ and (b) $G(|p|)$ corresponding to an eigenvalue $g_1g_2/(8\pi^2m) = 2.4986$ when $\Delta = -0.7$ and $k_1 = 1/2$.

$$r_{\text{lhs–rhs}} \equiv 1 - \frac{\frac{1}{2\mathcal{N}} \sum_{i=1}^{\mathcal{N}} \left[(\text{LHS}_i^a - \text{RHS}_i^a)^2 + (\text{LHS}_i^b - \text{RHS}_i^b)^2 \right]}{\frac{1}{2\mathcal{N}-1} \left[D^{(1)}_{\text{lhs–rhs}} - \frac{1}{2\mathcal{N}} D^{(2)}_{\text{lhs–rhs}} \right]}, \tag{3.16}$$

where

$$D^{(1)}_{\text{lhs–rhs}} = \sum_{i=1}^{\mathcal{N}} \left[(\text{LHS}_i^a + \text{RHS}_i^a)^2 + (\text{LHS}_i^b + \text{RHS}_i^b)^2 \right] \tag{3.17a}$$

and

$$D^{(2)}_{\text{lhs–rhs}} = \left[\sum_{i=1}^{\mathcal{N}} (\text{LHS}_i^a + \text{RHS}_i^a + \text{LHS}_i^b + \text{RHS}_i^b) \right]^2. \tag{3.17b}$$

A reliability coefficient $r_{\text{lhs–rhs}}$ of unity indicates that the left- and right-hand sides agree exactly at each point.

In Fig. 1, for $-0.95 \leqslant \Delta$ the solutions corresponding to the graphed eigenvalues all have reliability coefficients $r_{\text{lhs–rhs}} > 0.999999$. Although the number of basis functions is increased for Δ near minus one, constraints on computer time precluded obtaining equally accurate solutions for $-1. \leqslant \Delta < -0.95$: For solutions in the regions $-0.99 \leqslant \Delta < -0.95$ and $-1.0 \leqslant \Delta < -0.99$, the minimum reliability coefficients are 0.9993 and 0.99, respectively. The situation regarding reliability coefficients in Fig. 2 is similar.

As an additional check of each solution, from among the $\mathcal{N} = 20$ points where the left- and right-hand sides of the equations are calculated as part of the computation of the reliability coefficient, the locations where the absolute differences between the left- and right-hand sides of the equation are the greatest are printed as are the values of the left- and right-hand sides of the equation. In Fig. 1 for $-0.95 \leqslant \Delta$, the left- and right-hand sides almost always agree to at least four significant figures. For solutions in the region $-0.99 \leqslant \Delta < -0.95$, the left- and right-hand sides of the equation almost always agree to at least three significant figures. In the region $-1.0 \leqslant \Delta < -0.99$, for the least reliable solutions the worst disagreement between the left- and right-hand sides of the equation is about 25%.

4. Conclusions

The two-body, bound-state Bethe–Salpeter equation is solved numerically by converting it into a generalized matrix eigenvalue equation for the coupling constant. Although the coupling constant is real in the Lagrangian, it is usually very difficult to discretize the Bethe–Salpeter equation in such a way that the eigenvalues of the generalized matrix eigenvalue equation are all real. When it is possible, solutions are readily obtained. When is is not, it is still possible to obtain solutions in some, if not many, cases by expanding solutions in terms of basis functions that obey the boundary conditions satisfied by the solutions.

To demonstrate the utility of basis functions that obey the boundary conditions, a two-body, bound-state Bethe Bethe–Salpeter equation is solved for a situation where all eigenvalues of the corresponding generalized matrix eigenvalue equation are not real. Solutions are obtained in the zero-energy limit for a bound state of a spin-0 boson and a spin-1/2 fermion with unequal masses that interact via scalar electrodynamics and are described by the Bethe–Salpeter equation in the ladder approximation.

The equation can be discretized and solved using either the Rayleigh–Ritz–Galerkin method or the method of orthogonal polynomials. Here the method of orthogonal polynomials is used for two reasons: (1) All integrations can be performed analytically. (2) The original, unsuccessful analytical attempt to solve the equation used the method. After a Wick rotation, four-dimensional Euclidean space is projected onto the

surface of a unit, five-dimensional sphere. Solutions are then expanded in terms of linear combinations of hyperspherical harmonics in five-dimensional space, where each linear combination is chosen such that each basis function obeys the boundary conditions satisfied by the solution. Because the equation is rotationally invariant in four-dimensional space–time, it separates into two coupled equations in one variable. The equations are discretized by requiring that the coefficient of each spherical function on the left- and right-hand sides of the equation be equal. Although this method of discretization does not force all eigenvalues to be real, real eigenvalues are calculated. When a sufficient number of basis functions is used, the expansions corresponding to each real eigenvalue converge to a solution of the Bethe–Salpeter equation.

The possibility is currently being explored that the method used here can be used to obtain both zero-energy and finite-energy solutions to two-body, bound-state Bethe–Salpeter equations that have heretofore been intractable.

Acknowledgements

It is a pleasure to thank Professor Edward A. Overman II and Professor Cary B. Rader for very helpful discussions.

Appendix A. Calculation of expansion parameters

The parameters $a^{(3)}_{i,r,k}$ that appear in the expansion

$$\frac{1}{\cos^2(\theta/2)} P^{(3)}_{i,r}(\cos\theta) = \sum_{k=1}^{\infty} a^{(3)}_{i,r,k} P^{(3)}_{k-1+r,r}(\cos\theta) \tag{A.1}$$

are calculated analytically. Specifically, a recursion relation is first derived that allows $a^{(3)}_{i,r,k}, k \geqslant 2$, to be calculated in terms of i, r, k, and $a^{(3)}_{i,r,1}$. An analytical expression for the expansion parameter $a^{(3)}_{i,r,1}$ is then derived to complete the calculation.

To derive the recursion relation it is convenient to change to the variable $z = \cos\theta$ before multiplying both sides of (A.1) by $\cos^2(\theta/2) = \frac{1}{2}(1+z)$,

$$P^{(3)}_{i,r}(z) = \sum_{k=1}^{\infty} a^{(3)}_{i,r,k} \frac{1}{2}(1+z) P^{(3)}_{k-1+r,r}(z). \tag{A.2}$$

Using (A.23) in [5] to rewrite the right-hand side of the above equation solely in terms of spherical functions,

$$P^{(3)}_{i,r}(z) = \sum_{k=2}^{\infty} \frac{1}{2}\left[\frac{k+2r+1}{2k+2r+1} a^{(3)}_{i,r,k} + a^{(3)}_{i,r,k-1} + \frac{k-2}{2k+2r-3} a^{(3)}_{i,r,k-2}\right] P^{(3)}_{k+r-2,r}(z), \tag{A.3}$$

where $a^{(3)}_{i,r,0} \equiv 0$. The above equation immediately yields the desired recursion relation:

$$a^{(3)}_{i,r,k} = \frac{2k+2r+1}{k+2r+1}\left[2\delta_{k+r-2,i} - a^{(3)}_{i,r,k-1} - \frac{k-2}{2k+2r-3} a^{(3)}_{i,r,k-2}\right]. \tag{A.4}$$

An expression for $a^{(3)}_{i,r,k}$ is obtained by applying the orthogonality relationship (3.15) to (A.1),

$$a^{(3)}_{i,r,k} = \frac{(2k+2r+1)(k-1)!}{2(k+2r+1)!} \int_{-1}^{1} \mathrm{d}z\, 2(1-z) P^{(3)}_{k-1+r,r}(z) P^{(3)}_{i,r}(z). \tag{A.5}$$

The expansion parameter $a^{(3)}_{i,r,1}$ is calculated using (3.3) and

$$P^{(3)}_{r,r}(z) = \frac{(2r+1)!}{2^r r!}(1-z^2)^{r/2}, \tag{A.6}$$

which follows from (3.3). Thus, (A.5) becomes

$$a^{(3)}_{i,r,1} = \frac{(2r+3)}{(2r+2)2^r r!}\int_{-1}^{1} \mathrm{d}z(1-z)(1-z^2)^r \frac{\mathrm{d}^r}{\mathrm{d}z^r} C_i^{(3/2)}(z). \tag{A.7}$$

The above integral is evaluated using the generating function for Gegenbauer polynomials (see, for example [27])

$$(1-2zt+t^2)^{-3/2} = \sum_{i=0}^{\infty} C_i^{(3/2)}(z)t^i. \tag{A.8}$$

Multiplying both sides of (A.7) by t^i and summing over i

$$\sum_{i=0}^{\infty} a^{(3)}_{i,r,1}t^i = \frac{(2r+3)}{(2r+2)2^r r!}\int_{-1}^{1} \mathrm{d}z(1-z)(1-z^2)^r \frac{\mathrm{d}^r}{\mathrm{d}z^r}(1-2zt+t^2)^{-3/2}. \tag{A.9}$$

Taking the derivative of $(1-2zt+t^2)^{-3/2}$ r times with respect to z and rewriting the integral in terms of the variable θ, where $\cos\theta = z$,

$$\sum_{i=0}^{\infty} a^{(3)}_{i,r,1}t^i = \frac{(2r+3)(2r+1)!t^{r-1}}{(2r+2)2^{2r+1}(r!)^2}\left[-(t-1)^2\int_0^{\pi}\frac{\mathrm{d}\theta\sin^{2r+1}\theta}{(1-2t\cos\theta+t^2)^{\frac{2r+3}{2}}} + \int_0^{\pi}\frac{\mathrm{d}\theta\sin^{2r+1}\theta}{(1-2t\cos\theta+t^2)^{\frac{2r+1}{2}}}\right]. \tag{A.10}$$

The above integrals are evaluated using formula 3.665:2 in [28], yielding

$$\sum_{i=0}^{\infty} a^{(3)}_{i,r,1}t^i = \frac{2r+3}{r+1}\sum_{i=r}^{\infty}(-1)^{i-r}t^i. \tag{A.11}$$

The desired formula for $a^{(3)}_{i,r,1}$ immediately follows from (A.11)

$$a^{(3)}_{i,r,1} = \begin{cases} 0 & \text{if } i < r, \\ (-1)^{i-r}\frac{2r+3}{r+1} & \text{if } i \geqslant r. \end{cases} \tag{A.12}$$

References

[1] S. Godfrey, N. Isugur, Mesons in a relativised quark-model with chromodynamics, Phys. Rev. D 32 (1985) 189.
[2] S. Godfrey, The constituent quark-model-a status-report, Nuovo Cimento A 102 (1989) 1.
[3] W. Lucha, F.F. Schöberl, D. Gromes, Bound-states of quarks, Phys. Rep. 200 (1991) 127.
[4] A.J. Sommerer, J.R. Spence, J.P. Vary, Relativistic momentum–space wave-equations and meson spectroscopy, Phys. Rev. C 49 (1994) 513.
[5] G.B. Mainland, Electromagnetic binding of a minimally interacting, relativistic spin-0 and spin-1/2 constituent: zero four-momentum solutions, J. Math. Phys. 27 (1986) 1344.
[6] N. Arkani-Hamed, Y. Grossman, Light active and sterile neutrinos from compositeness, Phys. Lett. B 459 (1999) 179.
[7] J.C. Pati, A. Salam, J. Strathdee, Are quarks composite? Phys. Lett. B 59 (1975) 265.

[8] O.W. Greenberg, J. Sucher, A quantum structuredynamic model of quarks, leptons, weak vector bosons and higgs mesons, Phys. Lett. B 99 (1981) 339.
[9] W. Buchmuller, R.D. Pecci, T. Yanagida, Quarks and leptons as quasi nambu-goldstone fermions, Phys. Lett. B 124 (1983) 67.
[10] J.C. Pati, Dynamical symmetry-breaking through preons and the sizes of composite quarks and leptons, Phys. Rev. D 30 (1984) 1144.
[11] M.A. Luty, R.N. Mohapatra, A supersymmetric composite model of quarks and leptons, Phys. Lett. B 396 (1997) 161.
[12] E.E. Salpeter, H.A. Bethe, A relativistic equation for bound-state problems, Phys. Rev. 84 (1951) 1232.
[13] G.C. Wick, Properties of Bethe–Salpeter wave functions, Phys. Rev. 96 (1954) 1124.
[14] C. Schwartz, Solution of a Bethe–Salpeter equation, Phys. Rev. 137 (1964) 717.
[15] N. Setô, I. Fukui, Scalar–scalar ladder model in the unequal-mass case. i numerical evidence for the complex eigenvalues, Prog. Theor. Phys. 89 (1993) 205.
[16] T. Nieuwenhuis, J.A. Tijon, O(4) expansion of the ladder Bethe–Salpeter equation, Few-Body Systems 21 (1996) 167.
[17] R. Sugano, Y. Munakata, On the Bethe–Salpeter equation for the scalar–spinor particle system, Prog. Theor. Phys. 16 (1956) 532.
[18] G.B. Mainland, Numerical method for solving two-body, bound-state Bethe–Salpeter equations for unequal constituent masses, Few Body Systems 26 (1999) 27.
[19] L.M. Delves, J. Walsh, Numerical Solution of Integral Equations, Clarendon Press, Oxford, 1974.
[20] K.E. Atkinson, A Survey of Numerical Methods for the Solution of Fredholm Integral Equations of the Second Kind, SIAM, Philadelphia, 1976.
[21] F.B. Hildebrand, Methods of Applied Mathematics, second ed., Prentice-Hall, Englewood Cliffs, NJ, 1965.
[22] J.D. Bjorken, S.D. Drell, Relativistic Quantum Fields, McGraw Hill, New York, 1965.
[23] E. Hecke, Über orthogonal-invariante integralgleichungen, Math. Ann. 78 (1918) 398.
[24] V. Fock, Zur theorie des wasserstoffatoms, Z. Phys. 98 (1935) 145.
[25] M. Levy, Wave equations in momentum space, Proc. R. Soc. London Ser., A 204 (1950) 145.
[26] B.J. Winer, Statistical Principles in Experimental Design, McGraw Hill, New York, 1962.
[27] W. Magnus, F. Oberhettinger, R.P. Soni, Formulas and Theorems for the Special Functions of Mathematical Physics, Springer-Verlag, Berlin, 1966.
[28] I.S. Gradshteyn, I.M. Ryzhik, Tables of Integrals, Series, and Products, Academic Press, New York, 1965.